



Low-frequency components and modulation processes in compressible cavity flows

N. Delprat *

Université Pierre et Marie Curie, Paris and LIMSI-CNRS, BP 133, Orsay Cedex 91403, France

ARTICLE INFO

Article history:

Received 13 March 2009

Received in revised form

11 May 2010

Accepted 13 May 2010

Handling Editor: R.E. Musafir

Available online 9 June 2010

ABSTRACT

The modulated character of cavity-flow oscillations is investigated through a so-called modulation analysis of spectral distributions. The approach is based on a recently proposed viewpoint on the Rossiter formula and concerns mid- to high-subsonic flows in shallow cavities. For this type of configuration, the spectra are mainly characterized by the presence of several dominant peaks (Rossiter modes) that are not in a harmonic relation but uniformly spaced at a distance equal to the fundamental frequency of the oscillation mechanism (aero-acoustic feedback loop). This feature is interpreted as the result of an amplitude modulation process and related to variations in the vortex–corner interaction in the downstream part of the cavity (γ modulation). A lower frequency modulation is identified through the secondary peak distribution. A detailed analysis of the spectral structure confirms the presence of a component at the corresponding frequency value (Δ_f mode). The assumption of a specific coupling between the two modulation processes is investigated. It leads to a new approximate form for the γ -modulation ratio that allows an explicit expression of the Rossiter constant γ related to aspect ratio of the cavity (L/D).

© 2010 Elsevier Ltd. All rights reserved.

1. Introduction

In a wide variety of configurations, self-sustained oscillations can occur in the shear layer developing above an open cavity. This unsteady but very coherent mechanism is due to a strong coupling between upstream and downstream dynamics of the flow, initiated by vortex–corner interactions at impingement and maintained through a complex feedback process [1–3]. In compressible high-speed flows, the feedback or upstream influence is of acoustic nature and Rossiter [4] first detailed its role, referring to previous works on the jet–edge interaction [5,6]. The cycle of events responsible for cavity oscillations is modeled as follows: small flow disturbances are convected downstream and amplified in the shear layer spanning the cavity. Their interaction with the downstream corner gives rise to acoustic waves that propagate upstream inside the cavity at sound speed and excite further disturbances in the sensitive region near shear-layer separation. For the oscillations to be self-sustained, the loop formed by the downstream-convected instabilities and upstream-propagating acoustic waves must be phase-locked. Hence, release of new vortices at the upstream corner and generation of acoustic disturbances at the cavity trailing edge must be coupled.

The phase coherence imposed by the locking condition yields a self-selection process of admissible frequencies. In particular, each of the oscillation modes must satisfy a given overall phase difference between the two cavity corners. It also explains the occurrence of jumps in frequency between successive oscillation stages [5] when freestream velocity or cavity length [4,7] is varied. These features are common to most flows with self-sustained oscillations in different

* Tel.: +33 1 69 85 81 54; fax: +33 1 69 85 80 88.

E-mail address: nathalie.delprat@limsi.fr

configurations (e.g. edge tone, impinging jet, cavity flow, pipe-cavity system [8]). Thus, the empirical relations established for frequency prediction have the same generic form (feedback-type relation) [2,9] and usually depend on some numerical constants deduced from the best fit to experimental data. In the Rossiter formula, widely used for high-subsonic compressible flows past shallow cavities (length-to-depth ratios L/D greater than one), two empirical constants are required. The first one, namely κ , is related to phase speed of shear layer disturbances and represents the ratio of convection velocity of vortices to freestream velocity ($\kappa=U_d/U_\infty$). The second one, namely γ , is interpreted as a factor to account for the phase lag between impingement of a vortex and emission of acoustic waves at the downstream corner.

In contrast with clear predominance of a single frequency in purely hydrodynamic oscillations (i.e. completely dominated by shear layer instability [10,11]), several significant peaks that are not harmonically related are present in pressure spectra of high-speed cavity flows [4,12]. This non-harmonic aspect is expressed by means of the constant γ , whose determination permits modeling of the $n-\gamma$ form of frequency distribution (n mode number). The standard set of values ($\kappa=0.57$, $\gamma=0.25$) is found to provide a rather accurate estimation of data in a large number of experiments. Consequently, the Rossiter formula

$$f_n = \frac{U_\infty}{L} \frac{n-\gamma}{M+1/\kappa} \quad (1)$$

is a useful guide to identify the primary oscillation modes at a given flow Mach number ($M=U_\infty/c_0$).

On the basis of this identification, further investigations on the relationship between dominant peaks (referred to as Rossiter modes) and additional spectral components can be carried out. In particular, examination of potential nonlinear interactions between modes is of great interest for modeling and control purposes [13,14].

Earlier studies, mostly conducted in water, were carried out to learn more about the mechanisms giving rise to well-defined secondary components through nonlinear distortion of the fundamental frequency (higher harmonics) or nonlinear interactions of two primary components (sum and difference frequencies) [15,16]. As demonstrated by Knisely and Rockwell [7], origin and nature of these interactions can be established partly from flow visualization, spectral content study and bicoherence analysis results [17]. In their experiment, the generation of difference and sum modes was found to result from amplitude modulation of fundamental frequency of shear-layer instability by a low-frequency component having its source in the downstream vortex–corner interaction. These observations were confirmed by a high level of phase coupling between the two interacting frequencies and the resulting sum or difference modes. Many other combination modes can be produced through nonlinear interaction of two waves. As an example, intermodulation modes play an important role in the transition process from laminar to turbulent flow for non-impinging shear layers artificially excited [18,19]. Unsteady recirculating flow within the cavity may also contribute to spectral complexity through substantial low-frequency modulation of the shear layer [20,21]. In addition, fluctuations of sound speed or of vortex-convection velocity may also induce frequency modulations of the oscillation modes. Due to these nonlinear and time-varying aspects, any interpretation of multiple frequency content remains difficult and still incomplete.

The purpose of the present paper is twofold. The first is to report new insights gained by examining spectral distributions through a novel viewpoint on the Rossiter formula that we recently proposed [22]. The second is to investigate the role of the very low frequencies in the frame of this examination. Our approach differs from that of previous workers in the sense that the Rossiter formula is regarded as a spectral model of an amplitude modulation mechanism involving fundamental frequency of the aero-acoustic feedback loop and lower ones. The premise of this unusual interpretation is that the non-harmonic aspect of frequency distribution can be viewed as the result of a modulation process instead of the consequence of a phase lag. The relevance of this proposition has been tested on various experimental data available in existing literature and its effectiveness for mode identification and, to some extent, for nonlinear interaction analysis has been clearly demonstrated [22]. Recently, this signal-based model has been investigated by Malone et al. [23] on their own experimental data and its advantage for description of complex spectral distributions has been confirmed. They have also shown that new insight on variation of the Rossiter empirical parameters with Mach number can be obtained through the modulation analysis viewpoint.

The signal processing aspects that motivate our approach as well as significant findings of our preliminary investigation will be briefly reviewed in the following section. In order to avoid misunderstanding, some relevant quantities and new terms related to our Rossiter mode interpretation will be clarified. Then we will show how the proposed approach has naturally led us to focus on the presence of strong secondary peaks very close to the dominant ones as well as on existence of very low-frequency components with significant amplitudes. Both of these additional components have formerly received little attention, except in Kegerise et al. [13] and in recent numerical works (see [24] and its references). The question of their role in the cavity-flow oscillations and their possible relationship with the main amplitude modulation process will be discussed in the last section.

2. Modulation viewpoint

2.1. Spectral signature modeling

Fig. 1 schematically portrays Rossiter peak distribution at a given Mach number. It provides a simple but relevant illustration of the prominent spectral characteristics of cavity-flow oscillations, which are

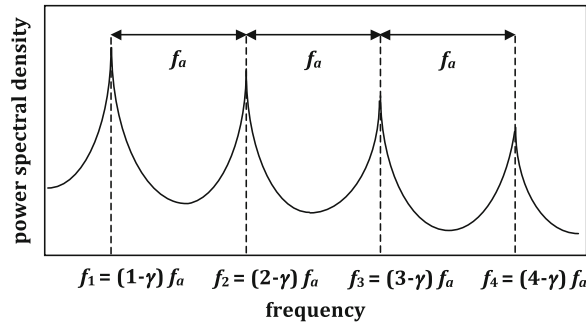


Fig. 1. Schematic diagram of spectral signature of cavity-flow oscillations as predicted by the Rossiter formula.

(i) a constant frequency interval f_a between successive components

$$f_a = f_{n+1} - f_n = \frac{U_\infty}{L} \frac{1}{M + 1/\kappa}, \quad n \text{ being an integer,} \tag{2}$$

(ii) a non-harmonic frequency distribution

$$f_n = (n - \gamma)f_a, \quad \gamma < 1. \tag{3}$$

Such characteristics are suggestive of an underlying modulation process. Indeed, defining γ as a frequency ratio in Eq. (1) allows interpreting the spectral signature as a sequence of difference frequencies

$$\begin{aligned} f_b &= \gamma f_a, \\ f_n &= n f_a - f_b. \end{aligned} \tag{4}$$

According to Rossiter's work, f_a represents the frequency of the aero-acoustic feedback loop formed by a vortex traveling across the cavity in time L/U_c and an acoustic wave propagating to the upstream corner in time L/c_0 :

$$f_a = \frac{1}{L/c_0 + L/U_c}, \tag{5}$$

with c_0 and U_c assumed to be constant within the cavity.

Consequently, when the frequencies of the Rossiter modes are non-harmonically distributed ($\gamma \neq 0$), they can be viewed as difference frequencies resulting from the interaction of a frequency f_a (or one of its harmonics) and a given lower one f_b . From this perspective, a two-step process combining nonlinear distortion and amplitude modulation of a periodic wave of frequency f_a can model the spectral signature. The first step yields generation of a harmonic sequence of components centered at $n f_a$ ($n \geq 1$). The second step gives rise to a global peak shifting of frequency f_b . Hence, it can be conjectured that non-harmonic frequency distribution of the Rossiter frequencies simply results from amplitude modulation of the aero-acoustic loop and that the rate of this modulation process is quantified by the value of γ [22].

As mentioned in the introduction, Knisely and Rockwell [7] already proposed interpretation of some spectral components in terms of amplitude modulation by a low-frequency component. In their water flow experiment, the modulating component of frequency α is related to cyclic variations of transverse displacement of the shear layer induced by vortex impingements at the downstream corner. Its nonlinear interaction with fundamental frequency of shear layer instability β produces a secondary peak at $\beta - \alpha$ (with $\alpha = 0.4\beta$ or 0.5β). Generally, amplitude of this difference component is much smaller than those of the two interacting ones. In the compressible case, the difference modes (Eq. (4)) predicted by the Rossiter formula are dominant peaks in amplitude. Moreover, fundamental or carrier frequency (f_a) and modulating frequency ($f_b = \gamma f_a$) are not present in the spectra (or with very small amplitudes). Hence, the Rossiter modes can be considered as survivors of a nonlinear interaction that will be not easily quantifiable except if f_a has significant amplitude. This case occurs in a few experimental configurations and will be commented in the following section.

2.2. Analyses of experimental spectra

This new viewpoint provides a useful investigatory tool for spectrum analysis, especially for complex distributions or when the standard set of empirical constants (γ, κ) does not give a satisfactory agreement with experimental data. Primary findings of our investigation through the proposed modulation analysis are reported below and somewhat generalized (for detailed examples based on experimental data, see [22,23]).

2.2.1. (γ, κ) estimates

Let us consider again the common case of a non-harmonic spectrum with three or four large-amplitude components, quasi-equally spaced as shown in Fig. 1. From Eq. (2), it easily follows that the constant κ can be directly estimated from

spectral analysis. For this aim, average value of frequency intervals between pairs of adjacent peaks is calculated as

$$(f_a)_{mean} = (f_{n+1} - f_n)_{mean}, \tag{5a}$$

where f_n is the measured frequency of the n th dominant peak. This gives an estimate of the fundamental frequency loop f_a and consequently of κ .

Referring to Eq. (4), the difference between $(f_a)_{mean}$ (or one of its harmonics of order n) and the n th Rossiter mode of frequency f_n corresponds to the average value of modulating frequency f_b :

$$(f_b)_{mean} = (f_{a,n})_{mean} \text{ where } (f_{a,n})_{mean} = n(f_a)_{mean} - f_n. \tag{6}$$

This simply allows determination of the constant γ as

$$\gamma = (f_b)_{mean} / (f_a)_{mean}. \tag{7}$$

Fig. 2 provides an overview of different steps of the estimation process. The agreement between measured Rossiter frequencies and the predicted ones was found to be generally within 1% or 2%.

2.2.2. Mode identification

Improvement in frequency prediction accuracy is the first implication of the proposed modeling. Critically speaking, the standard set of (γ, κ) values also provides satisfactory estimation with respect to experimental values (generally within 5–10%) when the dominant peaks are well defined and regularly spaced. The important point here is that the estimation process above described requires that particular attention be given to the global spectrum structure. Starting out with the analysis of the Rossiter peak distribution, relationships between spectral components (primary and secondary ones) are then interpreted on the basis of modulation features. This approach is quite similar to that of Miksad [18] and Miksad et al. [19] with regard to sideband structure interpretation in terms of amplitude and phase modulated carrier wave. Note however that in controlled transitions (free shear layer externally excited at two unstable frequencies), mode identification is much easier because interacting components (f_1, f_2) and their combination modes $(c_{n,p} = nf_1 \pm pf_2 \text{ with } n, p = 1, 2, 3, \dots)$ are simultaneously present in the spectral distribution, except near the transition stage close to final turbulent breakdown. Hence, the degree of phase coupling among $(f_1, f_2, c_{n,p})$ can be quantified with bispectral analysis and the nonlinear nature of wave interactions confirmed.

In our model, a similar coupling among (nf_a, f_b, f_n) is represented by Eq. (3). It expresses that any Rossiter mode of frequency f_n originates from the interaction of (nf_a, f_b) components. It is important to note that this coupling will be explicitly satisfied only if the fundamental loop frequency f_a is present in the spectrum with significant amplitude. In this case, the frequency relationship

$$f_a - f_{n+1} + f_n = 0, \tag{8}$$

where n is an integer, will be directly identified from experimental data. In other words, some spectral components will explicitly correspond to the sum or difference frequency of two dominant modes (that is, in fact, f_a and another Rossiter mode). As a result, a high degree of phase coupling will be detected for any (f_a, f_{n+1}, f_n) frequency triads. Such a singular case has few experimental illustrations. It appears however in one of the experiments of Kegerise et al. [13] ($M=0.4, L/D=2, R_e=1.5 \times 10^6$). For this configuration, we have established [22] that the first dominant component in the spectrum is the aero-acoustic loop frequency f_a and does not correspond to the first Rossiter frequency in the non-harmonic sequence predicted by the Rossiter formula (with $\gamma=0.25$). It is clear that the aero-acoustic loop frequency is associated with a cavity-flow mode and can be defined by the Rossiter formula, in the case where $\gamma=0$. In order to mark this difference, we propose to name it *the fundamental aero-acoustic mode* and to keep the terminology *Rossiter modes* for cavity-flow modes that result from an amplitude modulation process (that is $\gamma \neq 0$). Note that a fundamental aero-acoustic mode, some of its harmonics and Rossiter modes have also been identified for the ($M=0.35, L/D=4$) and ($M=0.6, L/D=4$) cavity-flow configurations in the paper by Malone et al. [23].

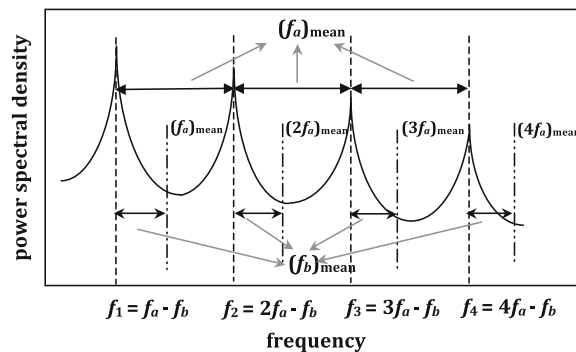


Fig. 2. Schematic diagram of (f_a, f_b) estimation from spectral data.

The identification of fundamental aero-acoustic and Rossiter frequencies in the same spectral distribution is worthy of note for two reasons. Firstly, it allows a plausible justification of unusual spectral relationships stressed by Kegerise et al., which were unexplained (cf Eq. (8)). Secondly, it could provide a finer characterization of the so-called mode-switching phenomenon [13,25] that corresponds to an alternation between two dominant modes. In effect, time–frequency analyses [13] show that, contrary to most flow configurations at high Reynolds numbers, change in the dominant mode is quite regular with time and always concerns the aero-acoustic loop mode and the third Rossiter mode. For this reason, one can speculate on the existence of a possible intermittent cycle between unmodulated ($\gamma=0$) and modulated ($\gamma\neq 0$) oscillation states, which could result in the occurrence of mode competition.

2.2.3. Connections with physical modeling

Since Rossiter's empirical model of cavity-flow oscillations, many analytical models have been developed on the basis of a feedback loop mechanism in order to better understand the physical processes at hand (see for instance the paper by Tam and Block [26] and its references). Recently, new perspectives on the nature of the cavity-flow oscillations have been proposed by Rowley et al. [27,28] suggesting that the oscillations may not always be self-sustained but that they may be lightly damped resonances, excited by turbulent motions or external acoustic waves under some flow conditions. These experimental observations have been confirmed for low freestream velocities with the help of an analytical approach by Alvarez and Kerschen [29] and Alvarez et al. [30]. Their model, which is promising for flow control problems, provides a global physical description in combining scattering analyses for the two ends of the cavity and a modeling of the shear layer and acoustic near-field. Moreover, it does not require any empirical constants. However, the question of the nature of cavity-flow regimes (self-sustained oscillations or lightly damped resonances) remains a challenging issue today and further evidence is required to establish a criterion in order to determine it.

The proposed approach is completely separated and very different in its goals from these physics-based models. It could be identified as a phenomenological approach in the signal processing area, based on spectral signature modeling and specifically focused on the modulated character of cavity-flow oscillations. For these reasons, it is not expected to provide an effective physical model. However, it is a very useful and simple tool to provide some links between spectral data and physical mechanisms. In particular, intriguing results that are inexplicable on the basis of the usual Rossiter formula interpretation can be examined from a different perspective. As an illustration, we refer to the value $\gamma \approx 0$ found in a high subsonic flow ($M=0.8$) past a deep cavity ($L/D=0.42$) [31,32]. In this experiment, the spectral distribution is quasi-harmonic and the authors have shown that the cavity-flow modes are of a flow-acoustic nature. Therefore, they propose to extend the Rossiter formula to deep cavities by taking very low values for γ . In terms of modulation features, this result again provides another example of an unmodulated regime through the observation of fundamental aero-acoustic loop frequency and its harmonics. It is to be pointed out that these frequencies are associated with pressure signals recorded at the front wall of the cavity. Moreover, it is reported that weak amplitude modulation is detected by another sensor located below the downstream edge of the cavity. This remark highly suggests that the modulation process could not be maintained between the two cavity corners in this experiment.

These results are consistent with the idea that the empirical constant γ will not enter into the relation for feedback loop frequencies but might rather represent a kind of 'end correction' to account for local effects near the trailing edge [33]. As a result, the modulation mechanism can be viewed as a perturbation of the fundamental loop frequency due to a cyclic variation in downstream vortex–corner impingements. It induces an amplitude-modulated upstream influence, whose strength presumably depends on the L/D ratio value as well as on some flow parameters (for instance, thickness of the initial boundary layer). This leads to the complex issue of the potential role of the recirculating flow within the cavity in the process of modulation transmission to the upstream region [3,20]. On the one hand, the upward-oriented jetlike flow along cavity walls observed by Lin and Rockwell [21] may participate in this process. On the other hand, variability of events due to recirculation eddy dynamics inside the cavity may alter its effectiveness. If, as generally suspected [34], these two phenomena (vortex–corner impingements and recirculation flow) contribute to the modulated character of the shear layer, to what extent they are competing or coupled remains unknown.

3. Additional modulation mechanism

3.1. Very-low-frequency components and sidebands

Up to this point, we focused on distribution of the dominant spectral components associated with primary oscillation modes. As mentioned in Section 2.2, these components are not strictly equally spaced in most spectra. This is the reason why estimate of the fundamental loop frequency f_a is given by the average value of $(f_{n+1} - f_n)$ intervals. More surprising is that frequency deviation between these intervals is always of the same order (typically around 20 Hz), whatever the studied flow configuration. In examining this aspect, we turned our attention to the existence of closely adjacent peaks to the primary ones. These peaks have nearly the same amplitude (or are slightly lower) than the Rossiter peaks. A closer inspection of the spectra reveals that they are located at the same frequency interval. That interval, denoted Δ_f , exactly corresponds to the value of the above mentioned frequency deviation. As an illustration, Fig. 3 shows the spectrum obtained for a $L/D=4$ cavity [12] with $L=0.24$ m, $M=0.8$, $U_\infty=292$ m s⁻¹ and $Re=3.8 \times 10^6$. In this case, the distance

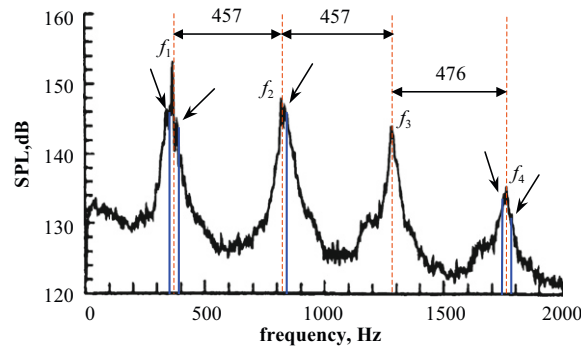


Fig. 3. Experimental spectrum obtained for a ($L/D=4$) cavity at $M=0.8$ [12]. Frequency intervals between the Rossiter modes (dotted vertical lines), some adjacent components with significant amplitudes (arrows) and Δ_f frequency deviation (solid vertical lines).

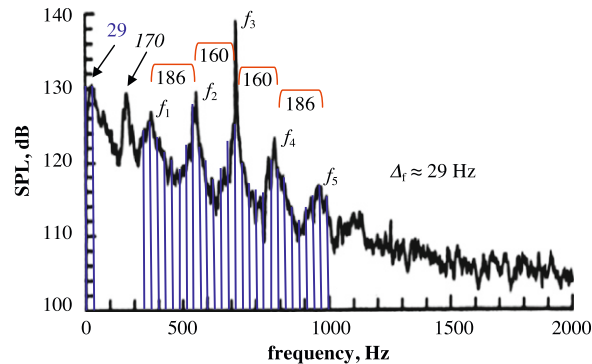


Fig. 4. Experimental spectrum obtained for a ($L/D=7$) cavity at $M=0.4$ [12]. Frequency intervals between the Rossiter modes and Δ_f intervals (solid vertical lines).

between two successive dominant peaks is equal to 457 and 476 Hz. Some additional components with significant amplitude can be clearly detected around the Rossiter peaks at intervals $\Delta_f \approx 476\text{--}457\text{ Hz} = 19\text{ Hz}$.

Of course, high resolution is required for discrimination of very close frequencies. The spectra under consideration were estimated with 2048 points FFTs and the frequency resolution is equal to 2.44 Hz [12]. Such a high resolution is not commonly used. When it is, little consideration is given to secondary peaks around the dominant ones. Usually, they are suspected to be caused by background noise rather than by a determined physical phenomenon. Yet, several spectral features suggest that they could result from modulation mechanisms at low frequency. In the first place, a well-defined component located at the Δ_f frequency is present in most studied spectra (cf Fig. 4). This very low-frequency component generally corresponds to the first peak in the spectral distribution. For instance, Kegerise et al. clearly notice its presence around 20 Hz in the spectrum obtained for a ($L/D=2$, $M=0.4$) cavity flow and around 15 Hz for a ($L/D=4$, $M=0.6$) one. Note that their spectral analyses were performed with a frequency resolution of about 5 Hz. Additionally, a noticeable band of Δ_f harmonics sometimes appears in the low-frequency part of the spectrum (see Fig. 6 in [13] for a clear illustration).

A second argument in favor of the existence of a low-frequency signal is that amplitude of the Δ_f component is generally significant compared with that of the Rossiter mode. As depicted in Fig. 4, it can even be higher than the amplitude of some dominant peaks. In the example ($L/D=7$, $M=0.4$) [12], the measured intervals between two successive Rossiter frequencies are found to be about 186 and 160 Hz. The low-frequency component is located at $\Delta_f \approx 29\text{ Hz}$ and secondary peaks are spaced at the same Δ_f value. One may notice that the Rossiter components appear to be very close to Δ_f harmonics (deviation of about 7 Hz on average). Since the Δ_f frequency is small, this feature could be coincidental and does not indicate the existence of a harmonic relationship. However, this remark will be of interest for schematic spectral modeling that will be detailed later. Note also the asymmetric aspect of upper and lower bands around the dominant peaks, which suggests the possible existence of both amplitude and frequency modulations (see [19] and references therein). Finally, it is to be pointed out that the peak at approximately 170 Hz is present in all spectra in the database, whatever the cavity length, for $M=0.4$. As reported by the authors, this component is probably not associated with cavity-flow resonance.

3.2. Low-frequency fluctuations and Rossiter mode modulations

As mentioned above, the existence of a peak at very low frequency was already pointed out in a few studies. In Kegerise et al. [13], time–frequency and bispectral analyses were performed to investigate possible connections between this peak

and observed amplitude modulation of the Rossiter components. It was clearly shown that the first dominant mode (f_a frequency in our analysis) experienced amplitude modulation at the Δ_f frequency while the other ones seemed to be modulated by different low frequencies. Moreover, frequency modulations can also be identified in the spectrograms of pressure signals. However, no significant coupling between the Rossiter modes and the Δ_f mode can be established by means of the bispectral analysis tools. In recent numerical investigations of three-dimensional (3D) cavity flows, Brès and Colonius [24] propose to relate the low-frequency mode to a three-dimensional centrifugal instability associated with recirculating vortical flow inside the cavity. Hence observed spanwise fluctuations of the shear layer can be primarily connected to the existence of this instability, whose modulating effect would depend on recirculating flow strength. From this perspective, the very-low-frequency modulation experienced by the Rossiter modes can arise from nonlinear interactions with the 3D mode. Their study also points out that the frequency value of this newly identified mode is little influenced by Mach number variation and is about an order of magnitude lower than that of the Rossiter mode.

We have noticed the same features for the Δ_f component. Typically, its value has been found to differ in frequency by about a few Hertz for different Mach numbers and the frequency ratio of Δ_f to that of the Rossiter first mode is around (1/10)–(1/20). These properties seem to corroborate the non-acoustic nature of the low-frequency mode and its plausible connection with the recirculation zone [24,35]. It is worthwhile noting that such a very low-frequency component was observed by Rockwell and Knisely [36] in spectra associated with water flows and interpreted as a supplementary modulation mechanism (in addition to the vortex–edge interaction ones), likely due to the recirculating vortex inside the cavity.

At present, physical origin of the very low-frequency modulation process remains an open question and it is not our purpose to further discuss it in this paper. Since the associated modulation process has been observed in various cavity-flow configurations by different authors, it seems to be of of interest however to extend the previous analysis in order to include its effects on the self-sustained oscillation mechanism. Whatever its nature (external noise or internal flow), the Δ_f modulation can combine with the Rossiter modes through two kinds of interaction: a global interaction that may alter coherence of the shear-layer (Rossiter) oscillations or a coupling with the fundamental aero-acoustic mode occurring before the γ -amplitude modulation process. In the second case, the Δ_f mode would bring modulation dynamics into the self-sustained oscillation mechanism itself. Thus, it would indirectly partake in mode modulation through its initial perturbation of the fundamental oscillation frequency. This simply implies that modulation parameters of both processes should be interrelated to generate spectral distributions with strong coherence and recognizably properties as observed for shallow cavity-flow tones.

4. Modulation combination hypothesis

In order to establish under which conditions both modulation process might be connected, a joint analysis of the Δ_f and γ -modulation parameters has to be performed. Due to the complexity of the task, we will restrict consideration to typical spectra where no singular feature is present. Spectral distribution of the ($L/D=4, M=0.8$) cavity flow described in the previous section is one such example and will be used as the reference spectrum. Its main characteristics in terms of frequency intervals and modulation ratios are reported in Table 1.

4.1. Schematic modeling of the Rossiter frequency distribution

4.1.1. Frequency ratios and position of spectral components

The fact that the modulating frequency Δ_f is the first spectral component in each studied spectra and that the Rossiter peaks are generally found to be very close to Δ_f harmonics provides some clues for spectrum modeling in terms of a modulation combination. Briefly, the idea is to interpret the Rossiter frequency distribution as the result of a frequency shift (γ modulation) of a frequency modulated wave whose components would be given by $nf_a \pm k\Delta_f$ (n harmonic number, k integer). This modeling is by no means unique and has to be regarded as an attempt to describe a possible scenario of modulation coupling, if it exists.

Let us first recall that for spectral distributions of type $f_c \pm kf_m$ the frequency position and spacing can be predicted by simply examining the so-called ratio of the modulating to carrier frequencies [37,38] denoted by $H=f_m/f_c$. For instance, if $H=N_2/N_1$ where N_1 and N_2 are integers with no common factors, the spectrum of the frequency modulated signal is harmonic and its fundamental frequency is given by

$$f_0 = f_c/N_1 = f_m/N_2. \tag{9}$$

Table 1

Δ_f and γ -modulation parameters extracted from the spectrum of the ($L/D=4, M=0.8$) cavity flow (cf Fig. 3). Mean values are in italics.

| f_a (Hz) | f_b (Hz) | Δ_f (Hz) | $\gamma = f_b/f_a$ | Δ_f/f_a | Δ_f/f_b |
|------------|------------|-----------------|--------------------|----------------|----------------|
| 462 | 98 | 19 | 0.21 | 0.041 | 0.194 |

In general, if H has the form $1/N$ with N any integer greater than 1 ($N_2=1$) then the fundamental is at the modulating frequency ($f_0=f_m$) and the carrier frequency is positioned at the N th harmonic of f_0 . In contrast, when $H=N$, where N is a positive integer greater than 1 ($N_1=1$), the fundamental frequency is equal to the carrier frequency ($f_0=f_c$). In both cases, if the ratio H approximates a simple value, that is to say N is replaced by $N'=N \pm \varepsilon$ ($\varepsilon < 1$), then the fundamental frequency is still at f_m/N_2 but the harmonics are shifted from their exact values by $\pm \varepsilon f_m$. Hence, when f_m is sufficiently small they can then be considered as pseudo-harmonics of the fundamental frequency f_0 . Lastly, note that modulation of a multicomponent and periodic carrier wave yields modulation of each of its harmonics by the same modulating frequency. In this case, sidebands are present around the carrier frequency f_c and its harmonics $n f_c$ at intervals of the modulating frequency f_m .

4.1.2. Pseudo-harmonic approximation

For the spectrum under consideration, the ratio H of Δ_f modulation is defined by $H=\Delta_f/f_a \approx 1/24$ with $\varepsilon=0.31$ (cf Table 1). For the sake of simplicity, the slight shift incurred for the components by the εf_m value (around 6 Hz) will be neglected for the moment. Note that this value is in the range of the average shift generally observed in the spectra (cf Fig. 4).

Under the pseudo-harmonicity approximation, it follows that $H=\Delta_f/f_a \approx 1/N$ with $N=24$:

$$f_a \approx N \Delta_f, \tag{10}$$

where N is an integer. Hence the multiple sidebands produced by the Δ_f modulation can be modeled by a harmonic series with modulating frequency Δ_f as the first spectral component ($f_0=\Delta_f$) and the fundamental oscillation frequency f_a localized at the N th harmonic. Obviously, Eq. (10) does not express that low-frequency fluctuations are essential to the development of shear layer oscillations. It simply allows us to predict the position of the f_a component with respect to the Δ_f component in the frequency distribution of the resulting modulated signal.

Since the γ modulation process operates a peak-shifting of the f_a frequency and its harmonics, harmonic aspect of the modeled spectrum will be preserved if and only if an integer ratio between the f_b and Δ_f values exists:

$$f_b \approx K \Delta_f, \tag{11}$$

K being an integer. As one may see, Table 1 indicates that the ratio of modulating frequencies Δ_f/f_b can be reasonably approximated by $1/5$ ($K=5$). It follows that

$$\gamma \approx f_b/f_a \approx K/N \approx 0.208 \tag{12}$$

and the Rossiter frequency distribution can be schematically modeled by

$$f_n = (n f_a - f_b) \approx (nN - K) \Delta_f, \tag{13}$$

where n is the mode number; N and K are integers.

As mentioned earlier, a similar type of modulation spectra, that is a multiple sideband distribution surrounding dominant components and a low-frequency component equal to the difference frequency between carrier and sidebands has been observed in controlled transitions of free shear layers to turbulence [18,19]. Although the source of this low-frequency mode may be different, the identification of spectral structure at low frequency expresses in both cases a sideband generation mechanism due to modulations of the fundamental mode and its harmonics. Within this context, Eq. (13) represents the idealized case of pseudo-harmonic relationships between the dominant peaks distribution and the sideband ones (cf Fig. 5). Experimentally, it is clear that the agreement between both distributions will greatly depend on the low-frequency value; the smaller the value, the better the agreement. For the spectrum under consideration, note that on average a shift of 7 Hz is found between the spectral data modeled with Eq. (13) ($N=24, K=5$) and experimental data. This shift is sufficiently small to support the assumption of pseudo-harmonicity and to carry on modeling on the basis of approximated Rossiter peak distribution.

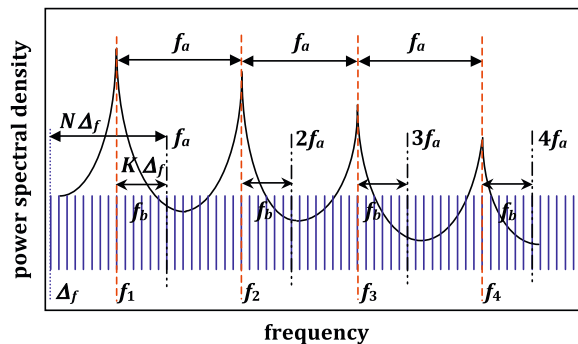


Fig. 5. Schematic diagram of the Rossiter peak distribution with respect to Δ_f distribution. Idealized case of a pseudo-harmonic distribution.

4.2. Approximate form for γ -modulation ratio

For the spectrum under consideration, one may remark that

$$N = K^2 - 1. \tag{14}$$

Therefore Eq. (12) can be simply written as

$$f_b/f_a \approx \frac{\sqrt{N+1}}{N}. \tag{15}$$

Since $\sqrt{N+1}$ is very close to \sqrt{N} , the f_b/f_a ratio can be approximated by

$$f_b/f_a \approx \frac{1}{\sqrt{N}} = 1/5 \approx \gamma. \tag{16}$$

It follows that

$$\Delta_f/f_b \approx \frac{1}{\sqrt{N}} \approx f_b/f_a \tag{17}$$

and

$$\Delta_f/f_a \approx 1/N \approx \gamma^2. \tag{18}$$

That is to say

$$\gamma \approx \sqrt{\Delta_f/f_a}. \tag{19}$$

Eq. (19) represents the approximate form for γ in the case when the ratio of modulating frequencies (Δ_f/f_b) is very close to the ratio of γ modulation (f_b/f_a). The loss of accuracy due to this approximation is not significant and is found to be less than 5% ($\gamma \approx 0.2$ instead of 0.21). More essential to the estimation order is the fact that Eq. (19) expresses the modulation process coupling through a specific relation between their modulation ratios. Note that this coupling would be consistent with observations made in the foregoing. In particular, the extent of peak shift caused by γ modulation would depend to a great part on the value of low-frequency fluctuations. Unlike the previous case, the correspondence between the modulating frequency ratio and the γ -modulation ratio (Eq. (17)) cannot be a priori justified from the spectrum structure. This point will be examined below.

4.3. Discussion on the new γ expression

4.3.1. Application to various spectral data and equality condition

When applied to other spectra, Eq. (19) provides estimates that are in good agreement with those calculated with the former procedure (cf Section 2.2.1). For instance, one may verify that for the ($L/D=2, M=0.4$) cavity flow [13] described in Section 2, Eq. (19) gives the approximated value $\gamma \approx 0.194$ ($\Delta_f \approx 18$ Hz, $f_a \approx 475$ Hz), which is very close to that obtained in our previous paper ($\gamma \approx 0.189$) [22]. To investigate the validity of this approximation for data distinct from the reference spectrum ones, a systematic study of the relationships between modulation ratios ($\Delta_f/f_a, f_b/f_a$) and value of the ratio of modulating frequencies Δ_f/f_b was performed. It clearly appeared that while Eq. (17) was not strictly satisfied (f_b/f_a and Δ_f/f_b are generally close but not equal), their mean value strikingly corresponded to the square root of Δ_f/f_a in every case. This is illustrated in Table 2 with modulation ratios of three different spectral distributions. In order to make the comparison easier, values of the inverse ratios have been listed.

Mathematically, this peculiar feature can be easily explained with the help of basic properties of the arithmetic and geometric means. Indeed, given two positive real numbers p and q , the following always holds:

$$\sqrt{pq} \leq \frac{p+q}{2}. \tag{20}$$

In other words, the geometric mean is always less than or equal to the arithmetic mean. Moreover, the equality condition of the inequality states that the two means are equal if and only if p and q are equal. Hence, taking $p=f_b/f_a$ and

Table 2

Relationships between modulation ratios $f_b/f_a, \Delta_f/f_a$ and modulating frequency ratio Δ_f/f_b for different configurations: (a) Kegerise et al. [13] experiment, (b) reference spectrum and (c) spectrum of Fig. 4. Note that $[\text{mean}]^{-1} = [(1/2)(f_b/f_a + \Delta_f/f_b)]^{-1}$.

| Configuration | $[f_b/f_a]^{-1}$ | $[\Delta_f/f_b]^{-1}$ | $[\text{mean}]^{-1}$ | $[\Delta_f/f_a]^{-1/2}$ |
|--------------------|------------------|-----------------------|----------------------|-------------------------|
| (a) $L/D=2, M=0.4$ | 5.28 | 5 | 5.135 | 5.137 |
| (b) $L/D=4, M=0.8$ | 4.71 | 5.16 | 4.926 | 4.931 |
| (c) $L/D=7, M=0.4$ | 2.28 | 2.62 | 2.436 | 2.442 |

$q = \Delta_f/f_b$ gives

$$\sqrt{\frac{f_b \Delta_f}{f_a f_b}} \leq \frac{1}{2} \left(\frac{f_b}{f_a} + \frac{\Delta_f}{f_b} \right). \quad (21)$$

That is to say

$$\sqrt{\frac{\Delta_f}{f_a}} = \frac{f_b}{f_a} \quad (\text{a}) \quad \text{if and only if} \quad \frac{f_b}{f_a} = \frac{\Delta_f}{f_b} \quad (\text{b}). \quad (22)$$

Eq. (22) explains the approximate form obtained by means of schematic modeling of the spectrum structure in the previous section and suggests that Eqs. (17) and (19) were not fortuitous. Furthermore, it allows us to validate the use of the new γ expression for different kinds of spectral data, provided the equality condition (22b) is satisfied.

4.3.2. Theoretical agreement and modulation compatibility

At this stage, one may consider that Eq. (19) simply expresses an algebraic property of modulation ratios. Its advantage is to give an additional way to estimate the γ value that is less complicated than the former procedure. Theoretically, the agreement between both estimates will depend on the equality condition; the closer the f_b/f_a and Δ_f/f_b , the better the agreement. In practice, the ability to accurately identify the low-frequency mode in the spectrum may improve it. For instance, for the ($L/D=2$, $M=0.4$) spectral distribution analyzed above, the difference between both estimates tends to zero when $\Delta_f \approx 18$ Hz ($\gamma \approx 0.194$) is replaced by $\Delta_f \approx 17$ Hz ($\gamma \approx 0.189$). In this case, note that $[\Delta_f/f_b]^{-1} \approx 5.29$ becomes quasi-equal to $[f_b/f_a]^{-1} \approx 5.28$ (see Table 3). Hence, small deviations in frequency estimates and/or slight variations in the physical phenomenon could explain why the equality condition is generally found to be satisfied under an approximate form (Eq. (17)) rather than strictly verified (Eq. (22)). Note also that a frequency shift of Δ_f within ± 5 Hz leads to significant changes in Δ_f/f_b and Eq. (17) no longer holds.

With respect to the proposed spectrum modeling, parts (a) and (b) in Eq. (22) express the modulation process coupling in a different form, even though they represent the same algebraic equality. Part (a) provides a relationship between modulation ratios (f_b/f_a and Δ_f/f_b). Part (b) shows that the modulation ratio characterizing the Rossiter mode distribution (f_b/f_a) might be determined by the ratio of the modulating frequencies (Δ_f/f_b). At present, it is not possible to establish whether or not the equality condition is physically relevant. However, we believe that if the modulation mechanisms were not interrelated, there would be small chance that the oscillation system generates modulating frequencies satisfying the same equation for different cavity-flow configurations. We recall that the f_b and Δ_f values have been estimated at first in a separate way, are not of the same order and supposed to be related to different mechanisms. Hence, it is not unreasonable to argue that Eq. (17) might reflect physical constraints linked to the cavity-flow properties. These constraints remain to be experimentally evidenced and it is clear that more experimental data have to be analyzed in order to corroborate this link for various Mach numbers and cavity aspect ratios.

To conclude, with regard to the proposed scenario, the equality condition may be naturally interpreted as a compatibility condition required for reinforcement and coherence of the modulation combination. Note that this condition does not necessarily yield a harmonic relationship between the Rossiter modes and the Δ_f components. Their conjunction will primarily depend on the form of γ ratio. It requires that $\gamma^2 = 1/k^2$ with $k=1/p=1/q$ integer. For instance, the relation is trivially verified for $\gamma=0.2$ ($1/p=1/q=5$) or $\gamma=0.25$ ($1/p=1/q=4$). This remark validates the pseudo-harmonicity approximation used for the modeling of the reference spectrum ($\gamma \approx 0.21$).

4.4. γ modulation and cavity aspect ratio

4.4.1. Modulation coefficient

Another interesting feature of the approximate form of the γ ratio is to provide a possible expression for γ dependence with respect to the cavity aspect ratio L/D and flow parameters. To date, this dependence has not been yet analytically established and γ values empirically found by Rossiter are still used as reference values. Taking non-dimensional frequencies (Strouhal numbers) in Eq. (19), we derived an explicit form for variation of γ with L/D . Indeed, as modeled by the Rossiter formula (Eq. (1)), the length scale characterizing the dominant modes is the cavity length L . Thus, the Rossiter frequencies are usually converted to Strouhal numbers in the form fL/U_∞ . Obviously, the same remark can be made for the

Table 3

Modulation ratios f_b/f_a and modulating frequency ratios Δ_f/f_b calculated for different Δ_f values. In italics, values estimated from the spectrum.

| Configuration | Δ_f (Hz) | $[f_b/f_a]^{-1}$ | $[\Delta_f/f_b]^{-1}$ |
|---------------------|-----------------|------------------|-----------------------|
| <i>L/D=2, M=0.4</i> | 23 | | 3.91 |
| | 18 | 5.28 | 5 |
| | 17 | | 5.29 |
| | 13 | | 6.92 |

fundamental frequency f_a (cf Eq. (2)). Following the findings of Brès and Colonius [39] and with reference to our earlier results, the Strouhal number related to the very low-frequency mode is defined as fD/U_∞ , where D is the cavity depth. Let $St_a = f_a L/U_\infty$ and $St_\Delta = \Delta_f D/U_\infty$ denote these numbers. We have

$$\gamma \approx \sqrt{\frac{St_\Delta}{St_a}} \sqrt{\frac{L}{D}} \tag{23}$$

Hence the link between cavity parameters and primary modulation of the fundamental oscillation mechanism can be modeled as a function of the square root of cavity aspect ratio modulated by a coefficient related to flow parameters. For the sake of clarity, denote $\sqrt{(St_\Delta/St_a)}$ by C_m (modulation coefficient). It follows that

$$\gamma \approx C_m \sqrt{\frac{L}{D}} \tag{24}$$

Eq. (24) is most appropriate to study the relative influence of cavity geometry on the modulation mechanism with respect to the fundamental aero-acoustic coupling. In particular, it could help examine how this influence might be balanced by low-frequency fluctuations inside the cavity (St_Δ value) as well as by the Mach number value $St_a \approx 1/(M+1/\kappa)$.

4.4.2. Dependence on flow parameters

As a simple illustration, let us consider the spectral data of Fig. 3 ($L/D=4, M=0.8$). We have

$$St_\Delta = 3.9 \times 10^{-3} \quad \text{and} \quad St_a = 3.8 \times 10^{-1}. \tag{25}$$

That is

$$C_m \approx 1.01 \times 10^{-1} \quad \text{and} \quad \gamma \approx 1.01 \sqrt{L/D} \times 10^{-1} \approx 0.202 \quad \text{for} \quad \sqrt{L/D} = 2. \tag{26}$$

In contrast, for the spectrum of Fig. 4 ($L/D=7, M=0.4$), we have

$$St_\Delta = 1.1 \times 10^{-2} \quad \text{and} \quad St_a = 4.64 \times 10^{-1}. \tag{27}$$

That is

$$C_m \approx 1.54 \times 10^{-1} \quad \text{and} \quad \gamma \approx 1.54 \sqrt{L/D} \times 10^{-1} \approx 0.41 \quad \text{for} \quad \sqrt{L/D} \approx 2.64. \tag{28}$$

Firstly, it is to be pointed out that the value of C_m coefficient is always an order of magnitude lower than the L/D square root in both cases (cf Table 4). This leads to a γ value necessarily smaller than one, as usually observed.

Then it is worthwhile to note that while the variation of Δ_f value induces a noticeable change in the St_Δ number, the variation in f_a value yields a smaller change in the St_a number. It also appears that the increase in modulation coefficient C_m (about 34%) is higher than that in the cavity aspect ratio (about 24%). Hence, the increase of γ value between the $L/D=4$ and $L/D=7$ cavity configurations seems to mainly result from the increase in the St_Δ number. Note that the C_m values listed in Table 4 are consistent with those directly calculated from the γ values proposed by Rossiter [4]. As shown in Table 5, deviation from the square root value increases with respect to the cavity aspect ratio in the same range. In accordance with the supposed link between the very low-frequency mode and recirculation zone unsteadiness, this change might provide a quantitative estimation of the influence of recirculating flow on shear layer modulation. Finally, it is to be pointed out that slight variations in the γ value with respect to Mach number at a fixed cavity ratio have been explicitly demonstrated by Malone et al. [23] from their experimental data, supporting the proposed hypothesis of γ dependence on flow parameters.

Table 4

Value of γ calculated from C_m and $\sqrt{L/D}$ for the ($L/D=4, M=0.8$) and ($L/D=7, M=0.4$) cavity flows [12].

| L/D | $\sqrt{L/D}$ | St_a | St_Δ | C_m | γ |
|-------|--------------|----------------------|----------------------|-------|----------|
| 4 | 2 | 3.8×10^{-1} | 3.9×10^{-3} | 0.101 | 0.202 |
| 7 | 2.64 | 4.6×10^{-1} | 1.1×10^{-2} | 0.154 | 0.41 |

Table 5

Average values of constant γ for different L/D ratios (cf Rossiter [4]). C_m is calculated from the value of γ .

| L/D | 4 | 6 | 8 |
|----------------------------|-------|-------|-------|
| γ_{Rossiter} | 0.25 | 0.38 | 0.54 |
| $\sqrt{L/D}$ | 2 | 2.56 | 2.82 |
| C_m | 0.125 | 0.155 | 0.191 |

This preliminary study clearly shows the possible implications of the modulation combination hypothesis. Obviously, it calls for an exhaustive examination of the relationships between the flow characteristics and the modulation parameters for different cavity-flow configurations to be substantiated. This examination lies outside the scope of the current paper and deserves a separate careful consideration. We will simply point out that while the main dependence of St_a number on Mach number is already modeled by the definition of the fundamental aero-acoustic loop frequency (cf Eq. (2)), the explicit form of St_a number dependence on flow parameters remains to be established. As reported in recent works [24,39], some parameters such as the Reynolds number or the ratio of cavity length to initial boundary layer momentum thickness can modify the Δ_f mode properties. To account for these experimental or numerical observations and to connect them with specific spectral features will be essential for continued exploration of modulation mechanisms at hand.

5. Conclusion

Interpreting the Rossiter formula as a spectral model of a modulated feedback process provides a new and useful way of investigating the cavity-flow oscillations. Classically, these oscillations are viewed as two-dimensional and supposed to be sustained through an aero-acoustic loop between the two cavity corners. For strong two-dimensional organized flow (for instance, flows at high Mach number past a deep cavity), the oscillation modes are weakly modulated and clearly correspond to pseudo-harmonics of the fundamental aero-acoustic loop frequency f_a . For shallower cavities, the spectra generally exhibit dominant peaks that do not form a harmonic series. This non-harmonic aspect is assumed to result from an amplitude-modulation mechanism generated by cyclic variations in the downstream vortex-corner interaction. As a result, the empirical constant γ is defined as the ratio of the corresponding modulating to modulated frequency (f_b/f_a). The detailed information provided by the proposed modulation analysis allows accurate estimation of mean values of the γ modulation and fundamental oscillation frequencies. Furthermore, it reveals the existence of an additional modulation mechanism at a very low-frequency Δ_f . At present, the physical origin of this frequency remains to be established. However, due to its relation to flow parameters and dominant frequency values, it could be plausibly connected with the three-dimensional recirculating flow within the cavity.

Spectra calculated with high frequency resolution allow us to identify a significant peak located at Δ_f . This peak generally corresponds to the first spectral component in the spectrum. Moreover, an underlying structure at the Δ_f frequency clearly appears in some spectra. In order to examine the assumption of a specific interrelation between the modulation processes, a modeling of spectral structure related to both modulation parameters is performed from the data of a reference spectrum. It brings out the possible existence of a compatibility condition between the modulating frequency ratio (Δ_f/f_b) and the γ -modulation ratio (f_b/f_a). Under this condition, an approximate form for the Rossiter constant γ can be established. It provides an alternative and effective way of estimating γ for different cavity-flow configurations. Moreover, an explicit expression for γ dependence on L/D can be naturally derived from this approximation and might be useful for the investigation of the combined influence of flow parameters and cavity geometry on shear layer modulation.

Further investigations on physical properties of the Δ_f mode in conjunction with flow visualizations of various experiments are required to complete the study. They could help to fully assess the relevance of the modulation combination hypothesis. Nevertheless, the aforementioned findings point to the significance of low frequency components and secondary peaks in spectral distributions as well as to the interest of a joint analysis of modulation mechanisms observed in the shear layer and within the cavity.

Acknowledgments

The author would like to thank F. Lusseyran, L. Pastur, J. Basley and T. Faure for many stimulating discussions on the proposed approach and cavity-flow modeling. She also wishes to thank F. Plantevin and P. Carlès for their relevant comments on some signal processing aspects developed in this work.

References

- [1] D. Rockwell, E. Naudascher, Review: self-sustaining oscillations of flow past cavities, *Transactions of the ASME, Journal of Fluids Engineering* 100 (1978) 152–165.
- [2] D. Rockwell, Oscillations of impinging shear layers, *AIAA Journal* 21 (5) (1983) 645–664.
- [3] D. Rockwell, Vortex-body interactions, *Annual Review of Fluid Mechanics* 30 (1998) 199–227.
- [4] J.E. Rossiter, Wind-tunnel experiments on the flow over rectangular cavities at subsonic and transonic speeds, reports 3438, *Aeronautical Research Council* (1964) 1–32.
- [5] G.B. Brown, The vortex motion causing edge tones, *Proceedings of the Physical Society* 49 (1937).
- [6] A. Powell, On the edge tone, *Journal of the Acoustical Society of America* 33 (4) (1961) 315–409.
- [7] C. Knisely, D. Rockwell, Self-sustained low-frequency components in an impinging shear layer, *Journal of Fluid Mechanics* 116 (1982) 157–186.
- [8] P. Oshkai, D. Rockwell, M. Pollack, Shallow cavity flow tones: transformation from large- to small-scale modes, *Journal of Sound and Vibration* 280 (2005) 777–813.
- [9] C.-M. Ho., N. Nosseir, Dynamics of an impinging jet. Part 1: the feedback phenomenon, *Journal of Fluid Mechanics* 105 (1981) 119–142.
- [10] D. Rockwell, C. Knisely, The organized nature of flow impingement upon a corner, *Journal of Fluid Mechanics* 93 (1979) 413–432.
- [11] S. Ziada, D. Rockwell, Oscillations of an unstable mixing layer impinging upon an edge, *Journal of Fluid Mechanics* 124 (1982) 307–334.

- [12] M.B. Tracy, E.B. Plentovich, Cavity unsteady-pressure measurements at subsonic and transonic speeds, *NASA Technical Paper* 3669 (1997).
- [13] M.A. Kegerise, E.F. Spina, S. Garg, L.N. Cattafesta, Mode-switching and nonlinear effects in compressible flow over a cavity, *Physics of Fluids* 16 (3) (2004) 678–687.
- [14] X. Gloerfelt, C. Bogey, C. Bailly, Numerical investigation of the coexistence of multiple tones in flow-induced cavity noise, *Proceedings of the 9th AIAA/CEAS Aeroacoustics Conference*, AIAA Paper 2003-3234, 2003.
- [15] M. Lucas, D. Rockwell, Self-excited jet: upstream modulation and multiple frequencies, *Journal of Fluid Mechanics* 147 (1984) 333–352.
- [16] R. Kaykayoglu, D. Rockwell, Unstable jet–edge interaction. Part 2: multiple frequency pressure fields, *Journal of Fluid Mechanics* 169 (1986) 151–172.
- [17] M.R. Hajj, R.W. Miksad, E.J. Powers, Perspective: measurements and analyses of nonlinear wave interactions with higher-order spectral moments, *Journal of Fluids Engineering* 119 (1997) 3–13.
- [18] W.R. Miksad, Experiments on nonlinear interactions in the transition of a free shear layer, *Journal of Fluid Mechanics* 59 (1973) 1–21.
- [19] W.R. Miksad, F.L. Jones, E.J. Powers, Y.C. Kim, L. Khadra, Experiments on the role of amplitude and phase modulations during transition to turbulence, *Journal of Fluid Mechanics* 128 (1982) 1–29.
- [20] C.H. Kuo, S.H. Huang, Influence of flow path modification on oscillation of cavity shear layer, *Experiments in Fluids* 31 (2001) 162–178.
- [21] J.C. Lin, D. Rockwell, Organized oscillations of initially turbulent flow past a cavity, *AIAA Journal* 39 (6) (2001) 1139–1151.
- [22] N. Delprat, Rossiter's formula: a simple spectral model for a complex amplitude modulation process?, *Physics of Fluids* 18 (7) (2006) 071703
- [23] J. Malone, M. Debiasi, J. Little, M. Samimy, Analysis of the spectral relationships of cavity tones in subsonic resonant cavity flows, *Physics of Fluids* 21 (5) (2009) 055103.
- [24] G.A. Brès, T. Colonius, Direct simulations of three-dimensional cavity flows, *Proceedings of the 13th AIAA/CEAS Aeroacoustics Conference*, AIAA Paper 2007-3405, 2007.
- [25] X. Gloerfelt, C. Bogey, C. Bailly, Numerical evidence of mode-switching in the flow-induced oscillations by a cavity, *International Journal of Aeroacoustics* 2 (2) (2003) 99–123.
- [26] C.K.W. Tam, P.J.W. Block, On the tones and pressure oscillations induced by flow over rectangular cavities, *Journal of Fluid Mechanics* 89 (1978) 373–399.
- [27] C.W. Rowley, T. Colonius, A.J. Basu, On self-sustained oscillations in two-dimensional compressible flow over rectangular cavities, *Journal of Fluid Mechanics* 455 (2002) 315–346.
- [28] C.W. Rowley, D.R. Williams, T. Colonius, R.M. Murray, D.G. MacMynowski, Linear models for control of cavity oscillations, *Journal of Fluid Mechanics* 547 (2006) 317–330.
- [29] J.O. Alvarez, E.J. Kerschen, Influence of wind tunnel walls on cavity acoustic resonances, *Proceedings of the 11th AIAA/CEAS Aeroacoustics Conference*, Monterey, California, AIAA Paper 2005-2804, 2005.
- [30] J.O. Alvarez, E.J. Kerschen, A. Tumin, A theoretical model for cavity acoustic resonances in subsonic flow, *Proceedings of the 10th AIAA/CEAS Aeroacoustics Conference*, Manchester, United Kingdom, AIAA Paper 2004-2845, 2004.
- [31] L. Larchevêque, P. Sagaut, I. Mary, O. Labbé, P. Comte, Large-eddy simulation of a compressible flow past a deep cavity, *Physics of Fluids* 15 (1) (2003) 193–210.
- [32] N. Forestier, L. Jacquin, P. Geffroy, The mixing layer over a deep cavity at high subsonic speed, *Journal of Fluid Mechanics* 475 (2003) 101–145.
- [33] D.G. Crighton, The jet edge-tone feedback cycle; linear theory for the operating stages, *Journal of Fluid Mechanics* 234 (1992) 361–392.
- [34] J.C.F. Pereira, J.M.M. Sousa, Experimental and numerical investigation of flow oscillations in rectangular cavities, *Journal of Fluids Engineering* 117 (1995) 68–74.
- [35] K. Chang, G. Constantinescu, S. Park, Analysis of the flow and mass transfer processes for incompressible flow past an open cavity with laminar and a fully turbulent incoming boundary layer, *Journal of Fluid Mechanics* 561 (2006) 113–145.
- [36] D. Rockwell, C. Knisely, Vortex–edge interaction: mechanisms for generating low frequency components, *Physics of Fluids* 23 (2) (1980) 239–240.
- [37] G. De Poli, A tutorial on sound synthesis techniques, *Computer Music Journal* 7 (4) (1983) 8–26.
- [38] J. Chowning, The synthesis of complex audio spectra by means of frequency modulation, *Journal of the Audio Engineering Society* 21 (7) (1973) 526–534.
- [39] G.A. Brès, T. Colonius, Three dimensional instabilities in compressible flow over open cavities, *Journal of Fluid Mechanics* 599 (2008) 309–339.